Quality assessment of stereoscopic spectral images obtained with use acousto-optic diffraction in a single TeO_2 crystal

Vladislav Batshev[1,2], Alexander Machikhin[1] and Vitold Pozhar[1,2]

[1]Laboratory of Acousto-Optic Spectroscopy, Scientific and Technological Center of Unique Instrumentation, Russian Academy of Sciences; 15, Butlerova, Moscow, Russia, 117342
[2]Laser and Opto-Electronic Department, Bauman Moscow State Technical University; 5, 2[ya] Baumanskaya, Moscow, Russia, 105005

Abstract
In this paper we propose dual-channel acousto-optic (AO) tunable filter for 3D spectral imaging. Different constructions of such AO filter are considered, which depend on optical scheme, on beams configuration, on the combination of input angles. The most convenient constructions are indicated. The results of computer simulation and image quality analysis are presented.

Keywords
Acousto-optic interaction, optical spectral filtration, three-dimensional imaging, dual-channel acousto-optical tunable filter.

I. Introduction
Spectral imaging enables visualization of physical and chemical properties of objects in those wavelength ranges where their contrast against background is maximal. For this purpose, light is selected in the absorption, emission or fluorescence bands of the inspected object. There are many machine vision, remote sensing and other applications in which conventional two-dimensional (2D) spectral imaging is not enough, so studying the distribution of the spectral properties over the non-flat (3D) object surface is necessary [1]. 3D spectral imagers provide much more information about the location and shape of the object structural elements [2].

II. 3D acousto-optic spectral imaging
Acousto-optic (AO) filtration of stereoscopic light beams is a promising approach to 3D spectral imaging. Diversity of permissible propagation directions and polarizations of interacting optical and acoustic waves provides multiple options for simultaneous filtration of non-collimated stereoscopic pair beams [3]. A promising idea for stereoscopic AOTF implementation is use of wide-aperture (tangential) diffraction geometry of two beams on a single acoustic wave [3,4]. In this case, the propagation directions of incident beams are uniquely determined by the direction of acoustic wave propagation. The relationship between the propagation angle θ of incident light beam (Fig.1a) and orientation of the acoustic wave-vector **q**, which is defined by the crystal face cut angle γ, is shown in Fig.1b. Dashed line corresponds to diffraction of ordinary-polarized light (“*o*”→“*e*”), while solid line - to extraordinary-polarized light diffraction (“*e*”→“*o*”). For a chosen value of ultrasound orientation angle γ, there exist four corresponding angles θ: two of ordinary-polarized (θ_{O1} , θ_{O2}) and two of extraordinary-polarized incident light (θ_{E1} , θ_{E2}).

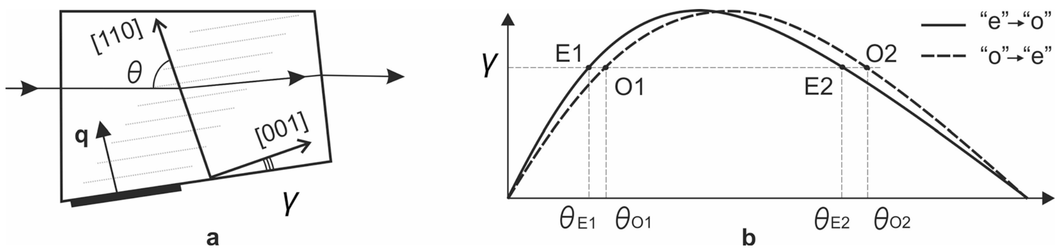

Fig.1. Light beam diffraction in AO cell made of TeO_2 (a)
and functional dependence $\gamma(\theta)$ in wide-aperture (tangential) diffraction geometry (b)

Due to typical requirements to AO figure-of-merit and limitations of acoustic walk-off, as well as to other reasons, the working angle γ is usually located in the range 6°..8°. We calculated all four θ angles corresponding to these typical angles γ in paratellurite (TeO_2) crystal (Table 1).

Table 1. Angles of ultrasound and light under wide-aperture AO diffraction

γ	θ_{E1}	θ_{O1}	θ_{E2}	θ_{O2}
6°	5.76°	6.56°	76.20°	77.84°
7°	6.75°	7.73°	73.85°	75.74°
8°	7.85°	8.93°	71.47°	73.61°

There are three basic configurations for beams propagation through AO cell: with parallel ($\theta_1 = \theta_2$), convergent ($\theta_1 \approx \theta_2$) and crossing ($\theta_1 \neq \theta_2$) beams. We denote these configurations as S-1, S-2 and S-3, correspondingly. Each of them suggests an individual shape of AO cell and the total construction of AOTF (Fig. 2).

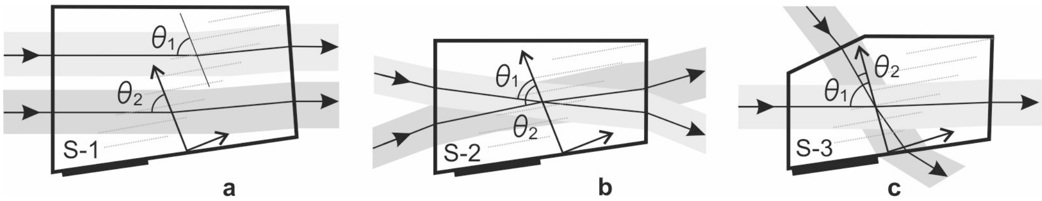

Fig.2. AO cell shapes in 3 beam configurations of stereo-imaging: parallel (a), convergent (b) and crossing (c)

Four choices of incident angles θ for both incident beams result in 16 combinations of diffraction geometries (Table 2). To distinguish between combinations, we denote them with pair of labels replicating indices of the first and second beams: for instance, "E1O2" means $\theta_1 = \theta_{E1}$, $\theta_2 = \theta_{O2}$. In fact, each of 16 combinations relates, in natural way, to certain of 3 optical configuration (Table 2). Therefore, we have to choose the optimum combination for each of three beam configurations.

Table 2. Beam configurations corresponding to incident angles combinations

	θ_{E1}	θ_{O1}	θ_{E2}	θ_{O2}
θ_{E1}	S-1	S-2	S-3	S-3
θ_{O1}	S-2	S-1	S-3	S-3
θ_{E2}	S-3	S-3	S-1	S-2
θ_{O2}	S-3	S-3	S-2	S-1

For accurate 3D reconstruction of the object shape in narrow spectral bands, AO filter must provide satisfactory quality of stereoscopic images within the whole tuning range. The image quality is reduced due to spatial and chromatic aberrations caused by AO diffraction. They demonstrate significant dependence on the cut angle of the wide-aperture filter [5]. Therefore, it is necessary to analyze all the aberrations thoroughly when choosing the best crystal shape and AOTF construction for 3D spectral imager. Below, we analyze every angle combination in three beam configurations in terms of aberrational characteristics of corresponding AO crystal cell. For this purpose, we use software Zemax with the program module [5] for ray tracing through the AO element.

Beam configuration S-1 (Fig. 2a) suggests a cell diffracting a pair of parallel beams. Its advantage is the same distortions of both beams so the optical systems forming the images in these beams may be identical. In addition, parallel beams simplify the output optical system design. The main disadvantage is large AO cell size necessary for spatial separation of the beams.

Beam configuration S-2 ensures small dimensions of the imager but have two drawbacks. Small angle between the beams results in rather complex design of input optical systems, which must be implemented, in form of a refractive biprism or a system of mirrors. The second issue is significant residual image aberrations because both beams are refracted on the same faces of AO cell so the aberrations of two beams can not be corrected simultaneously.

Beam configuration S-3 is unusual and needs careful elaboration, but it promises compact design and high image quality. The input optical system can be based on two flat mirrors with rather easy adjustment. The beams penetrate the AO cell through different faces so aberrations of each one can be corrected independently. It seems that "e"→"o" diffraction geometry (E1E2) is preferable because the beams are deflected upward, which facilitates slight decrease in AO cell size.

Therefore, the most promising are following geometries: O2O2 and E2E2 for S-1; E2O2 for S-2; E2E1 (which is equivalent to E1E2) for S-3 beam configurations (Table 3).

Table 3. Comparison of optimal diffraction geometry for different beam configurations

Beam configuration	Compactness	Feasibility of AO cell production	Ready solutions for entrance optics	Image aberrations mutual compensation
S-1	-	+	+	+
S-2	+	+	+/-	-
S-3	+	-	+/-	+

III. Aberration analysis

Besides the cell construction, a scheme for AO image spectral filtration also greatly affects the image quality [5]. Here, we discuss two main optical schemes of AO stereoscopic imagers - confocal (Fig. 3) and collimating (Fig. 4), and compare them in terms of the image quality. We analyzed both of them using S-2 beam configuration and E2O2 geometry with cut angle $\gamma = 7°$. Computer simulation was carried out separately for each of the stereoscopic channels. The image of nine points located at the nodes of a square grid was analyzed. Central point A is located on the optical axis. Point A′ is the image of the point A.

In the confocal scheme (Fig. 3) one can see the absence of chromatic drift and distortion. Therefore, at different wavelengths, the image magnification are almost identical. A detailed study of the spot diagram shows the presence of longitudinal chromatic shift, which appears as a small image defocusing when tuning the wavelength. Chromatic drift does not exceed 20 μm. Residual aberrations are also present, but their influence can be neglected, because the size of the scattering spot for the main wavelength 0.63 μm does not exceed the Airy diffraction circle, which is shown in white in all spot diagrams. Thus, the image quality in the confocal scheme can be considered high in both channels (Fig. 3a and b).

In collimating scheme (Fig. 4), the images get distorted in both channels. Due to distortion, the square is transformed into a curvilinear trapezium. Also, the chromatic drift is a significant. However, the quality of the monochromatic image is diffraction limited. It makes collimating scheme attractive for stereo imaging, since distortion and chromatic shift aberrations can be compensated by the calibration and further digital image processing.

IV. Results and discussion

In this research, we study the stereoscopic image quality provided by dual-channel AO filters made of TeO_2 crystal. We show that wide-aperture diffraction of two light beams on a single acoustic wave may be implemented using three different constructions of AO cell. Also, we compare two optical schemes of AO stereo imagers based on collimating and confocal optics.

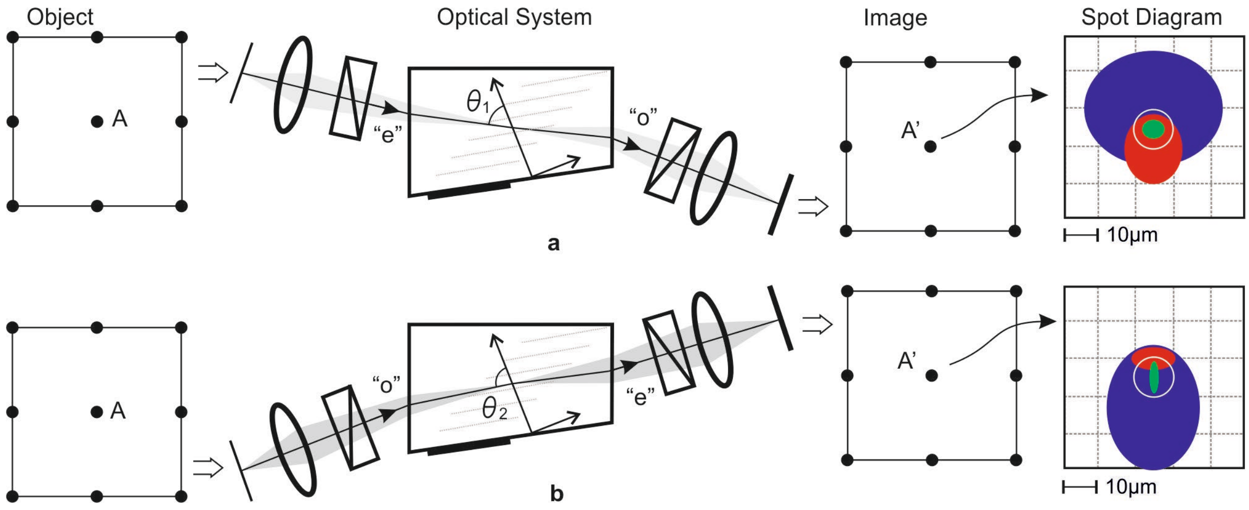

Fig. 3. Image aberrations in AO stereo imager based on confocal optical scheme

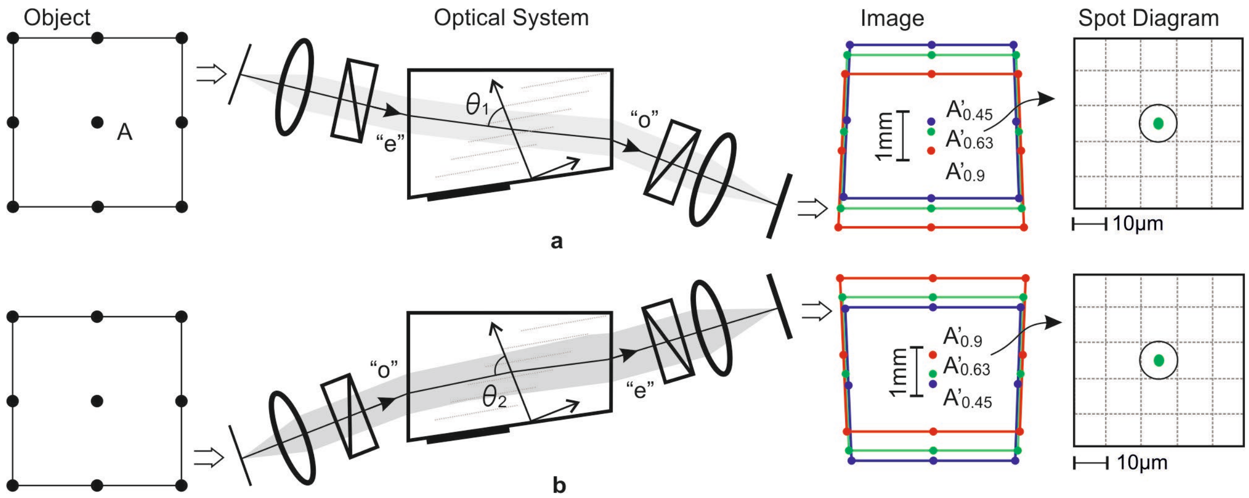

Fig. 4. Image aberrations in AO stereo imager based on collimating optical scheme

V. Conclusion

Rather good image quality in the considered schemes permit to conclude that it is possible to create a stereoscopic spectral imager based on a single AO crystal. Lens design of the spectral imager is not difficult due to the possibility of modeling of AO filter in the optical design software.

Acknowledgement

The work has been supported by the Russian Science Foundation (project 19-19-00606).

References

[1] A.S. Malik, T.S. Choi, H. Nisar. Depth Map and 3D Imaging Applications: Algorithms and Technologies, IGI Global (2011).
[2] M.H. Kim, T.A. Harvey, D.S. Kittle, H. Rushmeier, J. Dorsey, R.O. Prum, D.J. Brady. ACM Trans. on Graphics, 31(4), № 38 (2012).
[3] A.S. Machikhin, V.I. Batshev, V.E. Pozhar, A.A. Naumov, A.V. Gorevoy. Opt. Let., 43(5), 1087-1090 (2018).
[4] A.S. Machikhin, V.E. Pozhar. Tech. Phys. Let., 40(9), 823–826 (2014).
[5] A.S. Machikhin, V.I. Batshev, V.E. Pozhar. JOSA A, 34(7), 1109-1113 (2017).